第 24 卷第 3 期
2008 年 3 月

无 机 化 学 学 报
CHINESE JOURNAL OF INORGANIC CHEMISTRY

Vol.24 No.3
333~339

$M_5(PO_4)_3F$ (M=Ca,Sr,Ba)中 Sm^{3+}的电荷迁移态及 Sm^{3+}和 Eu^{3+}的电荷迁移能量关系

曾 取[1,2] 梁宏斌*[,1] 田梓峰[1] 林惠红[1] 苏 锵*[,1]
([1] 中山大学化学与化学工程学院, 广州 510275)
([2] 阳江职业技术学院, 阳江 529566)

摘要: 采用高温固相反应合成了 $M_{5-2x}Sm_xNa_x(PO_4)_3F$ (M=Ca,Sr,Ba)荧光体, 研究了其在真空紫外-可见光范围的发光特性。发现在 $Ca_5(PO_4)_3F$ 中 Sm^{3+}的电荷迁移带约在 191 nm, 在 $Sr_5(PO_4)_3F$ 中约在 199 nm, 而在 $Ba_5(PO_4)_3F$ 中约在 204 nm,随着被取代碱土离子半径的增大电荷迁移能量逐渐减小。比较了 $M_5(PO_4)_3F$ (M=Ca,Sr,Ba)中 Sm^{3+}和 Eu^{3+}电荷迁移能量的关系。

关键词: $Ca_5(PO_4)_3F$; $Sr_5(PO_4)_3F$; $Ba_5(PO_4)_3F$; Sm^{3+}; 电荷迁移态
中图分类号: O614.33; O614.23 **文献标识码**: A **文章编号**: 1001-4861(2008)03-0333-07

Charge Transfer States of Sm^{3+} and Charge Transfer Energy Relationship between Sm^{3+} and Eu^{3+} in $M_5(PO_4)_3F$ (M=Ca,Sr,Ba)

ZENG Qu[1,2] LIANG Hong-Bin*[,1] TIAN Zi-Feng[1] LIN Hui-Hong[1] SU Qiang*[,1]
([1]MOE Laboratory of Bioinorganic and Synthetic Chemistry, State Key Laboratory of Optoelectronic Materials and Technologies, School of Chemistry and Chemical Engineering, Sun Yat-sen University, Guangzhou 510275)
([2]Yangjiang Vocational And Technical College, Yangjiang, Guangdong 529566)

Abstract: The phosphors with general molecular formula $M_{5-2x}Sm_xNa_x(PO_4)_3F$ (M=Ca, Sr, Ba) were prepared by a high-temperature solid state reaction technique. The spectroscopic properties in VUV-Vis (vacuum ultraviolet-Visible)range were investigated. The maxima of CTBs (charge transfer bands) were found to be at about 191 nm for M=Ca, 199 nm for M=Sr, and 204 nm for M=Ba, showing the CT energy decreasing with the increase of the site size. The CT energy difference of Sm^{3+} and Eu^{3+} in a specific host lattice $M_5(PO_4)_3F$ (M=Ca, Sr, Ba) was compared. The relationships on the substituted ionic radii and the CT energy of Sm^{3+} and Eu^{3+} in $M_5(PO_4)_3F$ (M=Ca, Sr, Ba) are proposed.

Key words: $Ca_5(PO_4)_3F$; $Sr_5(PO_4)_3F$; $Ba_5(PO_4)_3F$; Sm^{3+}; CT states

The charge transfer (CT) from ligand atoms to lanthanide ions was first assigned in spectra by Jørgensen in 1960s[1]. During the past forty years, the CT states of lanthanide ions have been the subject of intense research, and the efficient phosphors on the basis of CT states of lanthanides have achieved practical application. Well-known and most successful examples are Eu^{3+} activated phosphors such as Y_2O_3:Eu^{3+} and Y(V,P)O_4:Eu^{3+} in tri-color lamps[2,3]. In these phosphors, the broad CT bands of Eu^{3+} ions are with the wavelength maximum near the wavelength of Hg vapor discharge (254 nm) in tri-color lamps, so CT states of Eu^{3+} ions

收稿日期: 2007-11-09。**收修改稿日期**: 2007-12-26。
国家自然科学基金(No.20571088),**广东省科技计划项目**(No.2005A10609001)**资助项目**。
* **通讯联系人**。E-mail: cesbin@mail.sysu.edu.cn
第一作者: 曾 取, 女, 34 岁, 副教授; 研究方向: 无机功能材料化学。

can efficiently absorb excitation energy and then convert 254 nm UV irradiation into red emission with higher quantum efficiency.

The primary interests of present investigation are from the following standpoints. First, the CT energy of Eu^{3+} is known to be the lowest among all trivalent lanthanides in a specific host, which is in UV-visible spectral region in general, so it is easy to be investigated. At the same time, because of the practical applications in tricolor phosphor lamps, the investigations on the CT states of Eu^{3+} ions in different matrices are promoted. In contrast, since with the higher CT energy for Sm^{3+} ion and the limitation of the experimental instrument setup, the investigation on Sm^{3+} CT energy is seldom to the best of our knowledge. Second, the maximum of CT band of Sm^{3+} ions in many wide band-gap matrices is expected to be at VUV (vacuum ultraviolet, wavelength λ<200 nm, energy E>50 000 cm^{-1}) or near VUV region. Phosphors excited by VUV light are now applied in technologies such as plasma display panels (PDPs) and mercury-free fluorescent lamps. The CT state occurs as broadband, it shows larger absorption cross-section than that of the narrow line-like f-f transitions, so it can absorb activation energy more efficiently. In our opinion, the broad CT band of Sm^{3+} might find application in searching novel phosphors for PDPs and mercury-free lamps. Third, as its high lying CT states in or near VUV range, Sm^{3+} ion is also expected to absorb activation energy and then efficiently transfer this energy to other lanthanides, Sm^{3+} ion can be used not only an activator but also a sensitizer for VUV phosphors. Efficient PDP or Hg-free lamp phosphors might be obtained by effective energy transfer from host to Sm^{3+} ions and finally to other activators. So it is important to investigate the CT states of Sm^{3+} in different host lattices.

Alkaline earth haloapatites $M_5(PO_4)_3X$ (M=Ca, Sr, Ba; X=F, Cl) are well known matrices of commercial phosphors $M_5(PO_4)_3X:Sb^{3+},Mn^{2+}$ in fluorescent lamps[2,3]. Some rare earth activated haloapatites have been explored[4~7] for their possible use as solid-state laser medium. To our knowledge, the CT states of Sm^{3+} in these hosts have not been reported in detail. So the spectroscopic properties of Sm^{3+} doped fluoroapatites $M_5(PO_4)_3F$ (M=Ca, Sr, Ba) are investigated and the positions of Sm^{3+} CT bands are reported in this paper.

1 Experimental

1.1 Samples preparation

A series of phosphors $M_{5-2x}Sm_xNa_x(PO_4)_3F$ (M=Ca, Sr, Ba; x=0.025, 0.05, 0.10, 0.15, 0.20, 0.25, 0.30, 0.35, 0.40) were prepared by a high-temperature solid state reaction technique. MCO_3 and $MHPO_4\cdot 2H_2O$ are taken as the sources of alkaline earth ions and PO_4^{3-} ions for M=Ca and Sr in $M_{5-2x}Sm_xNa_x(PO_4)_3F$. While for the preparation of $Ba_{5-2x}Sm_xNa_x(PO_4)_3F$, Ba^{2+} and PO_4^{3-} are from $Ba(NO_3)_2$ and $(NH_4)_2HPO_4$, respectively. F^- ions are provided by NH_4F (excess 10mol%) in $M_{5-2x}Sm_xNa_x(PO_4)_3F$. Since trivalent Sm^{3+} ions are located on divalent M^{2+} sites, Na^+ ions provided by Na_2CO_3 were added as a charge-compensating defect. Sm_2O_3 is of 99.99% pure grade, and all other chemicals were of A.R. (analytical reagent) grade. The stoichiometric mixtures of reactants were heated at 1 100 ℃ for 2 h under air atmosphere. The final products were obtained by washing the samples with distilled water and then drying. The reaction equations can be depicted as follows.

$$4(1-x)MCO_3 + 6MHPO_4\cdot 2H_2O + 2NH_4F + xSm_2O_3 + xNa_2CO_3 \xrightarrow{1\,373\ K/2\ h} 2M_{5-2x}Sm_xNa_x(PO_4)_3F + 2NH_3 + 16H_2O + (4-3x)CO_2, \text{ for } M = Ca, Sr$$

$$2(5-2x)Ba(NO_3)_2 + 6(NH_4)_2HPO_4 + 2NH_4F + xSm_2O_3 + xNa_2CO_3 \xrightarrow{1\,373\ K/2\ h} 2Ba_{5-2x}Sm_xNa_x(PO_4)_3F + 14NH_3 + 10H_2O + xCO_2 + 4(5-2x)NO_2 + (5-2x)O_2$$

1.2 Characterization

To check the purity of the phase, XRD patterns of the samples were recorded at room temperature (RT) on a Rigaku D/max 2200 vpc X-ray diffractometer with a copper anode (Kα radiation, λ=0.154 06 nm, U=20 kV, I=40 mA). The X-ray powder diffraction patterns of all un-doped and Sm^{3+}-doped samples are in agreement with the JCPDS standard data in PDF2 for $M(PO_4)_3F$ (M=Ca, Sr, Ba) (PDF#15-0876 for $Ca_5(PO_4)_3F$, PDF#50-1744 for $Sr_5(PO_4)_3F$, PDF#16-0803 for $Ba_5(PO_4)_3F$), indicating that the samples are pure hexagonal $M(PO_4)_3F$ phase.

The UV excitation and UV-excited emission spectra were recorded on a JOBIN YVON FL3-21 spectrofluorometer at room temperature and a 450 W xenon lamp was used as the excitation source.

The VUV excitation and corresponding luminescent spectra were measured at the VUV spectroscopy experimental station on beam line U24 of National Synchrotron Radiation Laboratory (NSRL). The electron energy of the storage ring is 800 MeV, and the beam current is about 150~250 mA. A Seya-Namioka monochromator (1 200 g·mm^{-1}, 100~400 nm) is used for the synchrotron radiation excitation photons, while an ARC-257 monochromator (1 200 g·mm^{-1}, 330~700 nm) for the emission photons, and the signal is detected by a Hamamatsu H5920-01 photomultiplier. The resolution of the instruments is about 0.2 nm. The pressure in the sample chamber is about 1×10^{-3} Pa. The relative VUV excitation intensities of the samples are corrected by dividing the measured excitation intensities of the samples with that of sodium salicylate(o-$C_6H_4OHCOONa$) in the same excitation conditions.

2 Results and Discussion

2.1 Luminescence of $Ca_5(PO_4)_3F$:Sm^{3+}

The UV excitation and UV-excited emission spectra of series samples $Ca_{5-2x}Sm_xNa_x(PO_4)_3F$ for x=0.025, 0.05, 0.10, 0.15, 0.20, 0.25, 0.30, and 0.35 were measured. No remark difference was found in the spectra of these samples, exception for the relative intensities. As an example, the spectra of sample $Ca_{5-2x}Sm_xNa_x(PO_4)_3F$ for x=0.20 are displayed in Fig.1.

The UV excitation spectrum in Fig.1 (a) shows several absorption lines by monitoring the emission at 599 nm. The ground state of Sm^{3+} ion is $^6H_{5/2}$ and the excitation peaks arise due to transitions from $^6H_{5/2}$ level to various excited states, which could be assigned easily on the basis of earlier work[8]. The absorption peak corresponding to the transition $^6H_{5/2}\rightarrow{}^4K_{11/2}$ at about 404 nm shows the maximum intensity, and some of the other transitions which appear with appreciable intensity are from ground state $^6H_{5/2}$ to excitation levels $^3H_{7/2}$(346 nm), $^4F_{3/2}$(363 nm), $^4D_{1/2}$(377 nm), $^5P_{3/2}+{}^6P_{3/2}$(418 nm), $^4G_{9/2}+{}^4I_{15/2}$ (438 nm), $^4F_{5/2}+{}^4M_{17/2}$(463 nm), and $^4I_{11/2}+{}^4I_{13/2}$ (474 nm).

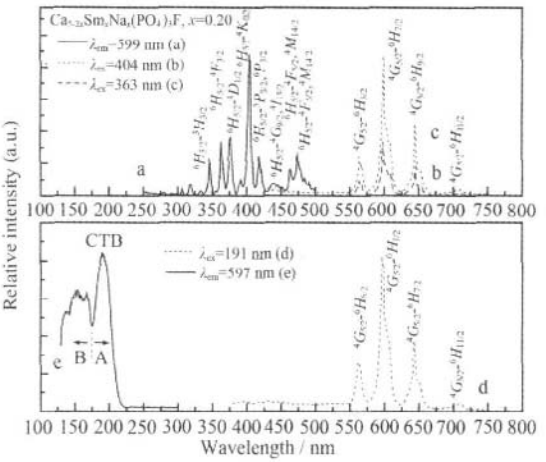

Fig.1 UV excitation spectrum (curve a, λ_{em}=599 nm), emission spectra under UV excitation (curves b and c, λ_{ex}=404, 363 nm), emission spectrum under VUV excitation (curve d, λ_{ex}=191 nm), and VUV excitation spectrum (curve e, λ_{em}=597 nm) for sample $Ca_{5-2x}Sm_xNa_x(PO_4)_3F$ (x=0.20) at RT

The emission spectrum of Sm^{3+} upon 404 nm $^6H_{5/2}$-$^4K_{11/2}$ excitation is shown in Fig.1 (b). The sample gives strong luminescence in the orange region with the calculated(CIE =Commission Internationale de L'Eclairage) chromaticity coordinates about x=0.58, and y=0.40. A similar spectrum is obtained with 363 nm $^6H_{5/2}$-$^3H_{7/2}$ excitation but the luminescent intensity is lower, as shown in Fig.1 (c). The emission peak due to the $^4G_{5/2}$-$^6H_{7/2}$ transition at about 599 nm appears very intense and seems to have two components. Similarly, the peaks near 564 nm($^4G_{5/2}$-$^6H_{5/2}$ transition) and 645 nm ($^4G_{5/2}$-$^6H_{9/2}$ transition) also shows two components. These components are most likely due to the Stark splitting of the ionic levels, though the possibility of transitions from $^4F_{3/2}$ and $^4G_{7/2}$ levels to some of the lower levels to give neighboring peaks cannot be ruled out. The $^4G_{5/2}$-$^6H_{11/2}$ transition at about 710 nm is very weak. The VUV-excited emission spectrum in Fig.1(d) shows same characteristics as UV-excited emission spectra in Fig.1(b, c).

The VUV excitation spectrum in Fig.1 (e) includes two parts. The absorption in part (A) is the charge transfer (CT) transition from ligand O^{2-} atoms to Sm^{3+}, and the dominant band is peaked around 191 nm, which corresponds to energy about 6.49 eV.

It is well known that the fluorapatites $M_5(PO_4)_3F$ (M=Ca, Sr, Ba) crystallize in the hexagonal system with

the space group corresponding to $P6_3/m$. Two types of M^{2+} ions occur in $M_5(PO_4)_3F$. The 40% of M^{2+} ions are labeled M(I) in Wyckoff 4f positions, which are with nine-fold oxygen coordination in high symmetry C_3 sites. In contrast, the 60 % of M^{2+} ions are labeled 6h M(II) in Wyckoff 6h positions, which are with six-fold oxygen and one-fold fluorine coordination in low symmetry C_s sites. Here we assume that the Sm^{3+} ions may preferentially enter Ca(II) sites in the host lattice. The seven-fold coordination Ca^{2+}/Sm^{3+} ions are reported to be with ionic radii 106/102 pm, whereas the nine-fold coordination Ca^{2+}/Sm^{3+} ions are 118/113 pm[9]. The ionic radius of Sm^{3+} is smaller than that of Ca^{2+} whenever seven or nine-fold coordination. Because the nine-fold coordination Ca(I) sites are larger than seven-fold coordination Ca(II) sites, the smaller Sm^{3+} ion tend to enter the smaller Ca(II) site. So the Ca(II) sites are dominantly occupied by Sm^{3+} ions.

The bands in part (B) are with wavelength shorter than 175 nm, and we consider that the absorptions in this range include the electronic excitation of anions PO_4^{3-} and the f~d transitions of Sm^{3+} in the host.

In our systematic work, we also prepared different rare earth ions, such as Ce^{3+}, Tb^{3+} and Dy^{3+} activated $Ca_5(PO_4)_3F$[10]. A broad band with a maximum at about 172/175/171 nm was found in the VUV excitation spectrum of $Ce^{3+}/Tb^{3+}/Dy^{3+}$ doped sample, respectively. The electronic excitation of anions PO_4^{3-} may show variable energy in different phosphate hosts, but we thought that in a specific host, the influence of different rare earth activators on this energy would be limited. As other rare earth ions doped $Ca_5(PO_4)_3F$ also present absorption around this range, we believe that the bands below 175 nm may contain the electronic excitation of anions PO_4^{3-} in the host.

The absorptions in part B may also contain the f~d transitions of Sm^{3+} in the host. This viewpoint can be confirmed in terms of the following facts.

In our work on Ce^{3+} doped $Ca_5(PO_4)_3F$, we found that the lowest 5d state for Ce^{3+} in Ca(II) sites was with the energy about $E^{Ce}=3.226\times10^4\ cm^{-1}$ (~310 nm). According to Dorenboss viewpoint[11], the energy decline (D value) of the lowest 5d state in the host $Ca_5(PO_4)_3F$ relative to that in free gaseous state will be calculated to be $D=49\,340-E^{Ce}=1.708\times10^4\ cm^{-1}$ in Ca(II) sites. Here the value 49 340 corresponds to the lowest 5d state energy of Ce^{3+} in free gaseous state.

We suggest that this D value is adopted by Sm^{3+} ions in the host lattice also. The lowest 5d state energy of Sm^{3+} in free gaseous state is corresponding to $7.584\times10^4\ cm^{-1}$[11], so the lowest 5d state energy of Sm^{3+} in Ca(II) site is estimated to be $E^{Sm}=7.584\times10^4-D=5.876\times10^4\ cm^{-1}$ (~170 nm). The estimate positions are in the range of part A.

We also measured the composition with the highest emission intensity by varying the content of Sm^{3+} ions in $Ca_{5-2x}Sm_xNa_x(PO_4)_3F$ samples. Fig.2 gives the dependence of the integral intensity of $^4G_{5/2}\rightarrow{}^6H_{7/2}$ emission on its doping concentration (x value) in $Ca_{5-2x}Sm_xNa_x(PO_4)_3F$. It can be found that the emission intensity increases with the increase of their concentrations (x) first, getting a maximum value around x=0.20~0.25, and then decreasing with increasing its content (x) because of the concentration quenching. Thus, the optimum concentration is x=0.20~0.25 for Sm^{3+} in the $Ca_{5-2x}Sm_xNa_x(PO_4)_3F$ samples.

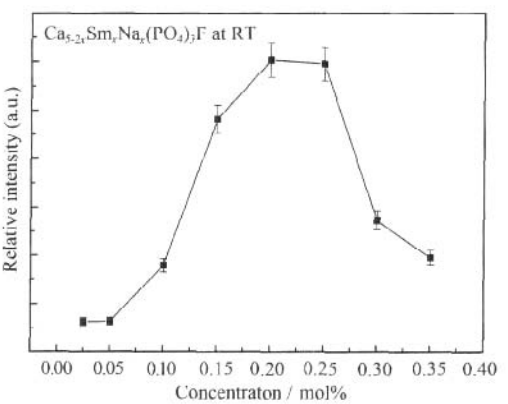

Fig.2 Relative $^4G_{5/2}\rightarrow{}^6H_{7/2}$ emission intensity as a function of Sm^{3+} concentration [xmol% value in $Ca_{5-2x}Sm_xNa_x(PO_4)_3F$] under 363 nm excitation at RT

2.2 Luminescence of $Sr_5(PO_4)_3F:Sm^{3+}$

The luminescence in the wavelength range between 520 nm and 2 840 nm for Sm^{3+} in $Sr_5(PO_4)_3F$ has been investigated [12]. Previous spectroscopic studies suggested that the majority of Sm^{3+} ions occupied the Sr(II) site having C_s symmetry[12]. In the present work,

the spectroscopic properties in the region 130~750 nm are investigated, and the results are exhibited in Fig.3. The UV excitation and UV-excited emission spectra for Sm^{3+} doped $Sr_5(PO_4)_3F$ in Fig.3(b~d) are in line with that for Sm^{3+} doped $Ca_5(PO_4)_3F$ in Fig.1(b~d), whose characteristics have been discussed in the above section. The VUV excitation spectrum in Fig.3(e) is also similar with that in Fig.1(e). The difference is found in the CT band positions. The CTB peaking is at about 199 nm (6.23 eV) in Fig.3(e), but it is about 191 nm (6.49 eV) in Fig.1(e), showing long-wavelength shift from Ca to Sr.

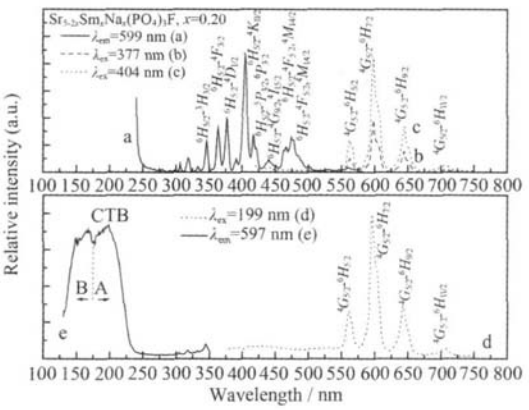

Fig.3　UV excitation spectrum (curve a, λ_{em}=599 nm), emission spectra under UV excitation (curves b and c, λ_{ex}=377 and 404 nm), emission spectrum under VUV excitation (curve d, λ_{ex}=199 nm), and VUV excitation spectrum (curve e, λ_{em}=597 nm) for sample $Sr_{5-2x}Sm_xNa_x(PO_4)_3F$ (x=0.20) at RT

When Sm^{3+} enter Sr(II) sites in $Sr_5(PO_4)_3F$ as that in $Ca_5(PO_4)_3F$, the decrease of CT energy from $Ca_5(PO_4)_3F$ to $Sr_5(PO_4)_3F$ can be understood in terms of the difference of the ionic radius of M^{2+} ions. The ionic radii Sr^{2+}> Ca^{2+}, so the site size of Sr(II) will be larger than that of Ca(II), resulting in the larger Sm-O bond distance for Sm^{3+} in Sr(II) sites than that in Ca(II) sites. Hence the CT transition for Sm^{3+} in $Sr_5(PO_4)_3F$ is with lower energy than that in $Ca_5(PO_4)_3F$.

Fig.4 shows the relative $^4G_{5/2}\rightarrow{}^6H_{7/2}$ emission intensity as a function of Sm^{3+} concentration [x value in $Sr_{5-2x}Sm_xNa_x(PO_4)_3F$] under 377 nm and 404 nm excitation at RT. The most intense emission intensity was found with the optimum concentration to be x=0.20 for Sm^{3+} in $Sr_{5-2x}Sm_xNa_x(PO_4)_3F$ whenever under 377 nm or 404 nm excitation.

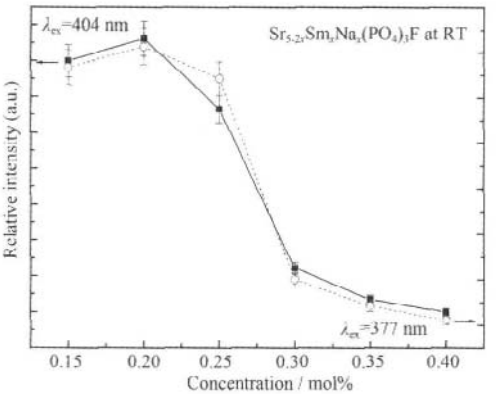

Fig.4　Relative $^4G_{5/2}\rightarrow{}^6H_{7/2}$ emission intensity as a function of Sm^{3+} concentration [$x$mol% value in $Sr_{5-2x}Sm_xNa_x(PO_4)_3F$] under 377 and 404 nm excitation at RT

2.3　Luminescence of $Ba_5(PO_4)_3F$:Sm^{3+}

The spectroscopic properties in 130~750 nm range for sample $Ba_{5-2x}Sm_xNa_x(PO_4)_3F$ (x=0.20) at RT are shown in Fig.5. The emission spectra in curves a, b and e and the UV excitation spectrum in curve c are similar with that in Figs.1 and 3, respectively. The CTB that observed in VUV excitation spectrum of Fig.5(d) is with a maximum at about 204 nm, which is due to the Sm^{3+} in Ba(II) sites.

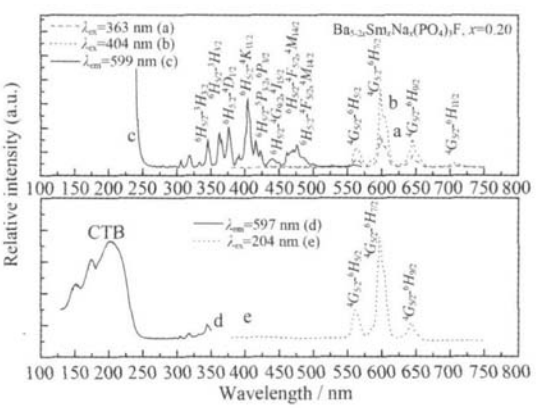

Fig.5　Emission spectra under UV excitation (curves a and b, λ_{ex}=363 and 404 nm), UV excitation spectrum (curve c, λ_{em}=599 nm), VUV excitation spectrum (curve d, λ_{em}=597 nm), and emission spectrum under 204 nm excitation (curve e) for sample $Ba_{5-2x}Sm_xNa_x(PO_4)_3F$ (x=0.20) at RT

For Sm^{3+} in M(II) sites, the coordination polyhedron is the same, but the electro-negativity decreases from Ca(1.00) to Sr(0.95) and Ba (0.89)[13]. According to this order, the ionicity degree of M(II)-O bond will be elevat-

ed and the covalency degree of M(II)-O bond will be decreased, so the CT energy of Eu^{3+} or Sm^{3+} will be increased from Ca(II) to Sr(II) and Ba(II). However, the experimental results indicate that the CT energy is decreased, which is contrary to the tendency of electronegativity values. This phenomenon directly suggests that the influence of electro-negativity of substituted ions on the CT energy is weak in this case. Other factor may decide the energy of CT band. As with the similar coordination environment for M(II) sites in $M_5(PO_4)_3F$, we think that ionic radius shows main influence on the CT energy of Sm^{3+} in M(II)sites. The ionic radius of nine-fold coordination $M(II)^{2+}$ increases from Ca(106 pm), to Sr(121 pm) and Ba(138 pm), the CT energy of Sm^{3+} decreases with the increasing of ionic radius. Furthermore, the following linear relationship could be obtained by fitting the experimental data,

$$E^{CT}(cm^{-1}) = 63\,600 - 108R \quad (1)$$

where E^{CT} is the CT energy of Sm^{3+} in the units of cm^{-1} and the ionic radius R of M^{2+} is in the units of pm. The fitted and the experimental CT energy values are listed and compared in Table 1, showing the experimental data are in agreement with the fitted values.

Table 1 CTB position (nm) of Sm^{3+} and Eu^{3+} and the CT energy difference ΔE (eV) between Sm^{3+} and Eu^{3+} in M(II) sites of $M_5(PO_4)_3F$

	$Ca_5(PO_4)_3F$		$Sr_5(PO_4)_3F$		$Ba_5(PO_4)_3F$	
	Found	Fitted	Found	Fitted	Found	Fitted
Sm^{3+}	191	192	199	198	204	205
Eu^{3+}	269	260	269	271	277	285
ΔE	1.88	1.69	1.62	1.69	1.60	1.69

2.4 Comparing the CT energies of Sm^{3+} and Eu^{3+} in $M_5(PO_4)_3F$

The $Eu^{3+}\leftarrow O^{2-}$ charge transfer band was reported to be around 260 nm in $Sr_5(PO_4)_3F$[14]. The CTBs of Eu^{3+} in $Ca_5(PO_4)_3F$ have also been depicted, and it was thought that the six excitation broad bands in 251~320 nm range are corresponding to the charge transfer transition of Eu^{3+}-ligand in different lattice sites with different charge compensating[7]. But the CT transition of Eu^{3+} in $Ba_5(PO_4)_3F$ has not been described to the best of our knowledge. Here we measure the excitation spectra of $M_{4.60}Eu_{0.20}Na_{0.20}(PO_4)_3F$ (M=Ca, Sr, Ba) under 616 nm emission at RT to verify the positions of $Eu^{3+}\leftarrow O^{2-}$ CT bands as displayed in Fig.7. The broad bands at about 269, 269, and 277 nm in Fig.7(a, b, c) are corresponding to the $Eu^{3+}\leftarrow O^{2-}$ CT transitions in $M_5(PO_4)_3F$, respectively. The results show that the CT energy of Eu^{3+} also increases with the substituted ionic size in principle, which is similar to that of Sm^{3+}. Fig.6(b) exhibits the change of Eu^{3+} CT energies in $M_5(PO_4)_3F$ (M=Ca, Sr, Ba) with the substituted M^{2+} ionic size. The experimental data are linear fitted to obtain the equation (2), by keeping the same slop with equation (1).

$$E^{CT}(cm^{-1}) = 49\,900 - 108R \quad (2)$$

where E^{CT} is the CT energy of Eu^{3+} in the units of cm^{-1} and the ionic radius R of M^{2+} is in the units of pm. The experimental data and the fitted values are listed in Table 1. The CT energy difference of Sm^{3+} is about 1.37×10^4 cm^{-1} (~1.69 eV) higher than that of Eu^{3+} in same host lattice. The CT energy difference of Sm^{3+} and Eu^{3+} in same lattice sites are statistically thought near 1.21 eV[15]. Our experimental result is somewhat larger than this value.

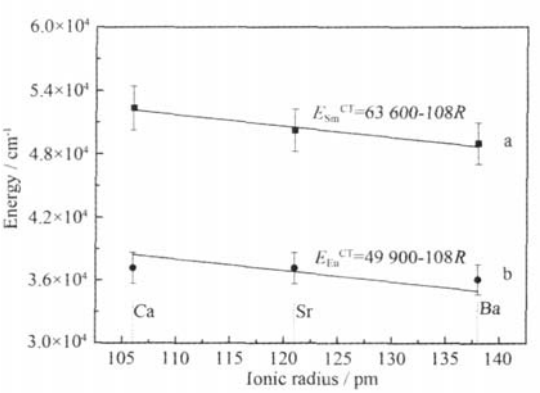

Fig.6 Relationship between the CT energies of Sm^{3+} and Eu^{3+} in $M_5(PO_4)_3F$ (M=Ca, Sr, Ba) and the ionic radius of M^{2+}

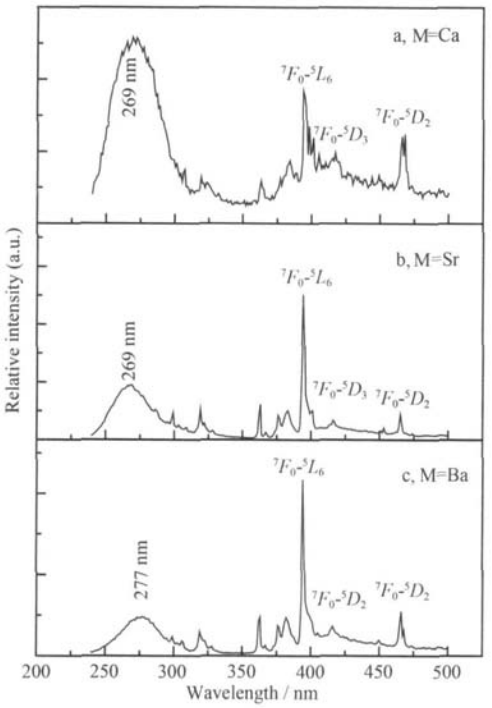

Fig.7　Excitation spectra and the position of Eu^{3+}←O^{2-} CT band in $M_{4.60}Eu_{0.20}Na_{0.20}(PO_4)_3F$ (M=Ca, Sr, Ba) detected at 616 nm at RT

3　Conclusions

Sm^{3+} activated phosphors $M_{5-2x}Sm_xNa_x(PO_4)_3F$ for M=Ca, Sr, Ba were prepared by a high-temperature solid state reaction technique. The charge transfer bands from O^{2-} ions in ligand to center Sm^{3+} ions were found to be at about 191 nm for M=Ca, 199 nm for M=Sr, and 204 nm for M=Ba. The substituted ionic size is considered to the main factor to decide the CT energy of Sm^{3+} in $M_5(PO_4)_3F$. A linear relationship between the CT energy of Sm^{3+}/Eu^{3+} and the ionic radius of substituted M^{2+} ions in the host lattices is suggested, which can be demonstrated to be E^{CT} (cm^{-1})=C- 108R, where the constant C=63 600 for Sm^{3+} and 49 900 for Eu^{3+}, and hence the CT energy difference of Sm^{3+} and Eu^{3+} in same lattice sites is near 1.69 eV.

Acknowledgments: The work is financially supported by the National Natural Science Foundation of China (Grant No. 20571088), by the Science and Technology Project of Guangdong province (Grant No.2005A10609001) and by a fund from Guangdong province Public Lab of Metal Materials.

References:

[1] Jorgensen C K. Mol. Phys., 1962,5:271
[2] Blasse G, Grabmaier B C. Luminescent Materials. Berlin: Springer-Verlag, 1994.116
[3] Shionoga S, Yen W M. Phosphor Handbook. Boston: CRC Press, 1999.
[4] Ryan F M, Warren R W, Murphy J, et al. J. Electrochem. Soc., 1978,125(9):1493~1498
[5] Fleet M E, Pan Y. J. Solid State Chem., 1994,112:78~81
[6] Dhiraj K S, Castano F. J. Appl. Phys., 2002,91(3):911~915
[7] Sahoo R, Bhattacharya S K, Debnath R. J. Solid State Chem., 2003,175:218~225
[8] Liu F S, Liu Q L, Liang J K, et al. J. Lumin., 2005,111: 61~68
[9] Shannon R D. Acta Cryst., 1976,A32:751~767
[10]Zeng Q, Liang H B, Dorenbos P, et al. J. Phys.: Condens. Matt., 2006,18(42):9549~9560
[11]Dorenbos P. J. Lumin., 2000,91:155~176
[12]Gruber J B, Zandi B, Merkle L D, et al. J. Appl. Phys., 1999, 86(8):4377~4382
[13]Lide R R. CRC Handbook of Chemistry and Physics 80th Edition. Boston: CRC Press Inc, 1999-2000.9~75
[14]Jagannathan R, Kutty T R N. J. Lumin., 1997,71:115~121
[15]Dorenbos P. J. Phys.: Condens. Matter., 2003,15:8417~8434